

Use of ^{11}C -MPDX and PET to Study Adenosine A_1 Receptor Occupancy by Nonradioactive Agonists and Antagonists

Soumen Paul¹, Shivashankar Khanapur¹, Jurgen W. Sijbesma¹, Kiichi Ishiwata², Philip H. Elsinga¹, Peter Meerlo³, Rudi A. Dierckx¹, and Aren van Waarde¹

¹Nuclear Medicine and Molecular Imaging, University Medical Center Groningen, University of Groningen, Groningen, The Netherlands; ²Research Team for Neuroimaging, Tokyo Metropolitan Institute of Gerontology, Tokyo, Japan; and ³Center for Behaviour and Neurosciences, University of Groningen, Groningen, The Netherlands

Adenosine A_1 receptors (A_1Rs) in human and rodent brains can be visualized with the radioligand 8-dicyclopropylmethyl-1- ^{11}C -methyl-3-propylxanthine (^{11}C -MPDX) and PET. Here we investigated whether A_1R occupancy by nonradioactive agonists and antagonists can be assessed with this technique. **Methods:** Small-animal PET scans with arterial blood sampling were obtained for 4 groups of isoflurane-anesthetized Wistar rats: controls ($n = 7$); pretreated with a centrally active A_1R agonist, N^6 -cyclopentyladenosine (CPA; 0.25 mg/kg intraperitoneally; dissociation constant, 0.48 nM; $n = 7$); pretreated with a moderate dose of caffeine (antagonist for A_1Rs and adenosine $\text{A}_{2\text{A}}$ receptors; 4 mg/kg intraperitoneally; dissociation constant, 11 μM ; $n = 6$); and pretreated with a high dose of caffeine (40 mg/kg intraperitoneally; $n = 6$). **Results:** The administration of CPA resulted in a strong reduction (>50%) in the heart rate, and caffeine administration resulted in a small increase (10%–15%). A caffeine dose of 4 mg/kg ($n = 6$) resulted in 65.9% A_1R occupancy, and a dose of 40 mg/kg ($n = 6$) resulted in 98.5% occupancy (calculated from a modified Lassen plot). However, the administration of CPA resulted in an increase in ^{11}C -MPDX binding in the brain. **Conclusion:** Small-animal PET with ^{11}C -MPDX can be used to assess antagonist but not agonist binding at A_1Rs . Changes in tracer uptake after the administration of CPA resembled previously reported changes induced by treatment of rats with ethanol and an adenosine kinase inhibitor (ABT702). Thus, the administration of an exogenous agonist or increasing the level of an endogenous agonist have similar effects. Agonists and antagonists may bind to different sites on the A_1R protein having allosteric interactions.

Key Words: adenosine A_1 receptor; occupancy; N^6 -cyclopentyladenosine; caffeine; brain

J Nucl Med 2014; 55:315–320

DOI: 10.2967/jnumed.113.130294

Adenosine A_1 receptors (A_1Rs) are G protein–coupled binding sites for the endogenous neuromodulator adenosine that inhibit the formation of the second messenger, cyclic adenosine monophosphate. They are implicated in the regulation of neuronal activity,

neuroprotection, and neuroinflammation (1). Some A_1R agonists may be beneficial in the treatment of atrial arrhythmias, type 2 diabetes, and angina (2).

Cerebral A_1Rs can be visualized with PET and radiolabeled xanthine antagonists, such as 8-dicyclopropylmethyl-1- ^{11}C -methyl-3-propylxanthine (^{11}C -MPDX) (3,4) and 8-cyclopentyl-3-[3- ^{18}F -fluoropropyl]-1-propylxanthine (^{18}F -CPFPX) (5,6). In a previous study, we reported that ^{11}C -MPDX and small-animal PET can be used to quantify regional A_1R densities in the rodent brain (7). PET offers unique opportunities for measuring the fraction of receptor populations occupied by nonradioactive drugs in the living brain and relating levels of occupancy to the magnitude of the therapeutic effect or to unwanted side effects. Receptor occupancy is estimated by assessing the competition of a nonradioactive drug and the radioligand for the same binding sites.

To explore the interaction of therapeutic drugs with A_1Rs , we treated rats with 2 test drugs before ^{11}C -MPDX small-animal PET scans: N^6 -cyclopentyladenosine (CPA) and caffeine. CPA is a potent adenosine receptor agonist (dissociation constant, 0.48 nM) with considerable selectivity for the A_1 subtype (8,9). Caffeine is a non-subtype-selective adenosine antagonist with moderate affinity (50% inhibitory concentration, 11–85 μM) and is widely consumed as a recreational drug (10,11). Occupancy of cerebral A_1Rs by caffeine or the potent (dissociation constant, 0.42 nM) and highly subtype-selective A_1R antagonist 8-cyclopentyl-1,3-dipropylxanthine (DPCPX) (12,13) has been visualized with the tracer ^{18}F -CPFPX (14,15) or ^{11}C -MPDX (7) and PET. However, PET studies of the occupancy of cerebral A_1Rs by agonists have never been reported. The findings of the present study, together with those of previous studies, indicate that dose-dependent occupancy of the A_1R population by antagonists can be assessed with PET. However, the administration of a high dose of the agonist CPA, which strongly decreases heart rate, body temperature, and locomotor activity in rodents (16), does not result in any measurable decline in binding of the PET tracer ^{11}C -MPDX in the rodent brain.

MATERIALS AND METHODS

(Radio)chemicals

CPA and caffeine were purchased from Sigma. The radioligand ^{11}C -MPDX was prepared as described previously (7).

Experimental Animals

All animal experiments were performed by licensed investigators in compliance with the Law on Animal Experiments of The Netherlands. The protocol was approved by the Committee on Animal Ethics of the University of Groningen. Male outbred Wistar–Unilever (specific-pathogen-free) rats

Received Aug. 1, 2013; revision accepted Oct. 17, 2013.

For correspondence or reprints contact: Aren van Waarde, Nuclear Medicine and Molecular Imaging, University Medical Center Groningen, University of Groningen, Hanzeplein 1, 9713GZ Groningen, The Netherlands.

E-mail: a.van.waarde@umcg.nl

Published online Jan. 16, 2014.

COPYRIGHT © 2014 by the Society of Nuclear Medicine and Molecular Imaging, Inc.

(body weight [mean \pm SD], 304 \pm 54 g) were obtained from Charles River, maintained with a 12-h light–12-h dark regimen, and fed standard laboratory chow ad libitum. Four groups of animals were studied: controls (pretreated with saline intraperitoneally; $n = 7$); pretreated with CPA (0.25 mg/kg intraperitoneally; dissolved in 0.3 mL of saline containing $<50 \mu\text{L}$ of dimethyl sulfoxide; $n = 7$) (16); pretreated with a moderate dose of caffeine (4 mg/kg intraperitoneally; dissolved in saline; $n = 6$); and pretreated with a high dose of caffeine (40 mg/kg intraperitoneally; dissolved in saline; $n = 6$). All treatments were given 5–10 min before injection of the tracer. Body weights and injected doses are shown in Table 1.

PET Scanning

Two rats were scanned simultaneously with a Focus 220 microPET (small-animal PET) camera (Siemens Medical Solutions). Animals were anesthetized with a mixture of isoflurane and air (ratio during induction, 5%; later reduced to $\leq 2\%$). Cannulas were placed in a femoral artery and vein for blood sampling and tracer injection, respectively. A transmission scan was obtained with an external source of radioactive cobalt to correct the subsequently acquired ^{11}C -MPDX emission images for attenuation and scatter. Rats were under anesthesia for 30–40 min before tracer injection (time required for cannulation and transmission scan). The tracer (^{11}C -MPDX; 21.5 \pm 9.7 MBq in a volume of 1 mL) was injected through the venous cannula, as a slow (1-min) bolus, with a Harvard-style pump. The camera was started as soon as the tracer entered the body of the first rat in the scanner; the second animal of the pair was injected 16 min later. Scanning was then continued for another 60 min. The animal that was injected second had also been anesthetized at a later time. Thus, the duration of anesthesia was similar in all study groups.

A list-mode protocol was used (76 min; brain in the field of view). A series of blood samples (18 samples; volume, 0.10–0.15 mL) were drawn, initially in rapid succession (5 s) and later at longer intervals (up to 30 min). Plasma was acquired from these samples by centrifugation (Eppendorf centrifuge; 5 min at 13,000 rpm). Radioactivity counts in 25 μL of plasma and 25 μL of whole blood were determined and used as an arterial input function. During the entire scanning procedure, the heart rate, stroke volume, and blood oxygen level of the animals were monitored with pulse oximeters (PulseSense; Nonin).

Analysis of PET Data

List-mode data were reframed into a dynamic sequence of 8 \times 30 s, 3 \times 60 s, 2 \times 120 s, 2 \times 180 s, 3 \times 300 s, 1 \times 480 s, 3 \times 600 s, and 1 \times 960 s frames. The data were reconstructed per time frame with an iterative reconstruction algorithm (attenuation-weighted 2-dimensional ordered-subset expectation maximization; provided by Siemens; 4 iterations; 16 subsets; zoom factor, 2). The final datasets consisted of 95 slices (slice thickness, 0.8 mm) and an in-plane image matrix of 128 \times 128 pixels (size, 1.1 mm). Datasets were fully corrected for random coincidences, scatter, and attenuation. Images were smoothed with a gaussian filter (1.35 mm in both directions).

Time–activity curves and volumes (cubic centimeters) for the areas of interest were calculated with Siemens Inveon Research Work Place 4.0 (IRW 4.0). A region of interest was drawn around the (entire) olfactory bulbs, frontal cortex, striatum, amygdala, parietal cortex, temporal cortex, occipital cortex, medulla, cerebellum, pons, and hippocampus in a template MR imaging scan that was coregistered with the PET scan of interest by image fusion (17). Standardized uptake values (SUVs) measured by PET were calculated with measured body weights and injected doses as follows: tissue activity concentration (MBq/mL)/[injected dose (MBq)/body weight (g)]. The cerebral volume of distribution (V_T) of the tracer was estimated either from a Logan plot (linear regression started 10 min after tracer injection) or from a 2-tissue-compartment model (2TCM) fit. For Logan graphic analysis, the blood volume was fixed at 3.6% (18). The partition coefficient (K_1/k_2) and the binding potential (k_3/k_4) of ^{11}C -MPDX were estimated from the model fit.

Because there is no region with negligible A_1R expression in the rodent brain, levels of receptor occupancy were calculated by comparing regional V_T s in control and drug-treated rats with a modified (i.e., axis-transformed) Lassen plot (19).

Biodistribution Studies

After the PET scan, the anesthetized animals were sacrificed. Blood was collected, and plasma was obtained from the blood sample by centrifugation (5 min at 1,000g). Several areas of the brain were dissected, and peripheral organs were excised. These tissue samples were weighed, and tissue radioactivity was measured by use of a γ counter with the application of decay correction. Tracer uptake was expressed as the dimensionless SUV.

Statistical Tests

Differences between groups were analyzed with a 1-way ANOVA. A probability of less than 0.05 was considered statistically significant.

RESULTS

Physiologic Responses to Drug Treatment

About 5 min after administration of the A_1R agonist CPA, a strong decline ($>50\%$) in the heart rate was noted. This decline persisted for the entire duration of the small-animal PET scan (60 min), although a slight return toward the baseline rate occurred near the end of the scan. The decline in the heart rate was accompanied by an increase in the cardiac stroke volume. Blood oxygenation levels were not significantly altered. The administration of caffeine resulted in a small increase (10%–15%) in the heart rate after 5 min; this increase persisted for the entire duration of the scan. There was no significant change in blood oxygenation levels.

Animal PET Images

The PET images acquired in the present study were similar to those reported previously (7). When animals were pretreated with

TABLE 1
Animal Data

Group	Body weight (g)	Injected dose	
		MBq	nmol
Control ($n = 7$)	311 \pm 56	23.3 \pm 4.0	2.1 \pm 0.4
CPA ($n = 7$)	312 \pm 31	25.7 \pm 5.5	2.4 \pm 0.5
Caffeine at 4 mg/kg ($n = 6$)	317 \pm 90	23.4 \pm 7.9	2.1 \pm 0.7
Caffeine at 40 mg/kg ($n = 6$)	275 \pm 19	12.1 \pm 13.8	1.1 \pm 1.3

Data are reported as mean \pm SD.

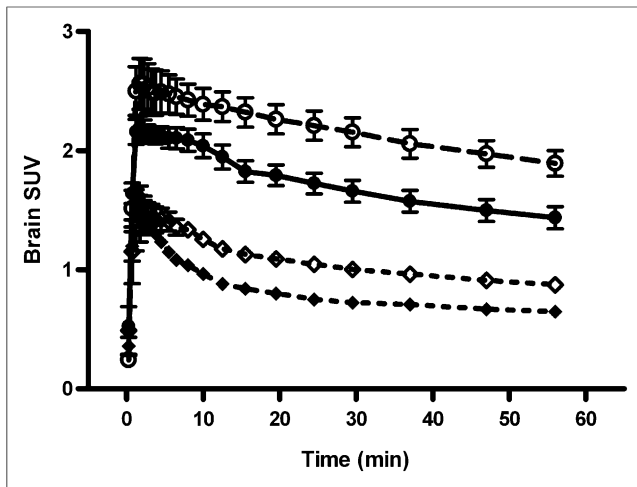


FIGURE 1. Kinetics of ^{11}C -MPDX-derived radioactivity in rat brain. Error bars indicate SEMs. ● = control animals; ○ = CPA-treated animals; ◇ = animals treated with caffeine at 4 mg/kg; ◆ = animals treated with caffeine at 40 mg/kg.

the A_1R agonist CPA, a global increase in tracer uptake relative to that observed in the control group was noted. After pretreatment of rats with caffeine (particularly at the high dose), cerebral uptake of the tracer was strongly reduced, and regional differences in tracer uptake were no longer apparent.

Kinetics of Radioactivity in Brain and Plasma

The cerebral kinetics of radioactivity in the present study were also similar to those reported previously (7). In rats pretreated with CPA, an increase in the uptake of radioactivity relative to that in the control group was noted (Fig. 1). In animals pretreated with caffeine, rapid washout of the tracer was observed, and the brain uptake of ^{11}C -MPDX was strongly reduced (Fig. 1).

The clearance of radioactivity from plasma appeared to be affected little by drug treatment. Although the shape of the plasma curve was different after treatment of animals with CPA, with a stronger initial increase in plasma radioactivity and then a greater decline (Fig. 2), areas under the curve were similar in the 4 treatment groups. Expressed as a percentage of the value for the control group, they were $92\% \pm 9\%$ (CPA), $112\% \pm 20\%$ (caffeine at 4 mg/kg), $104\% \pm 19\%$ (caffeine at 40 mg/kg), and $100\% \pm 16\%$ (saline-treated control). None of these differences was statistically significant.

Biodistribution Data

The biodistribution data acquired after the PET scan (Table 2) corresponded closely to the PET SUV data in the last scan frame.

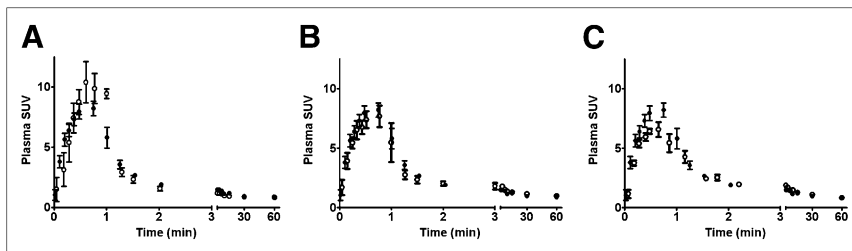


FIGURE 2. Kinetics of ^{11}C -MPDX-derived radioactivity in rat plasma. Error bars indicate SEMs. ● = control animals; ○ = animals treated with CPA (A), caffeine at 4 mg/kg (B), and caffeine at 40 mg/kg (C).

Treatment of rats with CPA did not result in any decrease but rather resulted in an increase in cerebral radioactivity. This increase was statistically significant in the amygdala, cerebellum, frontal cortex, hippocampus, medulla, parietal cortex, temporal cortex, occipital cortex, striatum, and the brain tissue left over after dissection. The increase noted in the entorhinal cortex and pons was not statistically significant because of a relatively large individual variance in the study groups. Outside the brain, tracer uptake was increased only in the liver (Table 2).

Pretreatment of animals with caffeine (4 mg/kg) reduced tracer uptake in the cingulate gyrus, entorhinal cortex, frontal cortex, hippocampus, medulla, and striatum. Among the peripheral organs, a significant reduction in tracer uptake was observed only in the spleen. Levels of radioactivity in the urine were increased (Table 2).

Pretreatment of rats with a high dose of caffeine (40 mg/kg) resulted in a highly significant reduction in tracer uptake in virtually all studied brain areas, with the exception of the pons and medulla (Table 2). Outside the brain, significant reductions in tracer uptake were noted in the spleen and duodenum, whereas uptake in the trachea was increased (Table 2).

Graphic Analysis of PET Data

The tracer V_T was calculated from a Logan plot, time-activity curves from a region of interest drawn around the entire brain, and radioactivity counts from arterial blood samples. Compared with the results for saline-treated controls, a significant increase in the V_T after pretreatment of animals with CPA (from 1.60 ± 0.23 to 2.38 ± 0.36 [$P = 0.0005$]) and a significant decrease after pretreatment with caffeine (from 1.60 ± 0.23 to 0.86 ± 0.08 [$P < 0.0001$] after a dose of 4 mg/kg and to 0.59 ± 0.06 [$P < 0.0001$] after a dose of 40 mg/kg) were seen (Fig. 3).

Compartment Modeling of PET Data

When a 2TCM was fitted to time-activity curves from a region of interest drawn around the entire brain, with radioactivity counts from arterial blood samples as the input function, the partition coefficient for ^{11}C -MPDX (K_1/k_2 ratio from the model fit) was found to be not significantly affected by CPA but significantly decreased after the treatment of animals with caffeine (Fig. 4). Receptor occupancy by caffeine—calculated with the formula $100 \times [(1 - k_3/k_4[\text{drug-treated}])/k_3/k_4(\text{control})]$ —for the dose of 4 mg/kg was 69.8%, and that for the dose of 40 mg/kg was 100%.

Tracer k_3/k_4 was significantly increased after treatment with CPA and significantly decreased by caffeine (Fig. 4). The PET data for the high-dose caffeine group were better fitted by a 1-tissue-compartment model (1TCM) than a 2TCM, in contrast to the data for the other 3 treatment groups. Blood volume could be left floating during the 2TCM or 1TCM fit. The value estimated by the fit program was $3.3\% \pm 0.4\%$ (mean \pm SEM; $n = 21$). However, in some animals, the program estimated a blood volume of 0%. Data for these animals are not included in the value reported for blood volume.

Estimation of Receptor Occupancy

Modified Lassen plots were prepared from the regional Logan V_T s for animals in the control, low-dose caffeine treatment, and high-dose caffeine treatment groups (Fig. 5). Both plots showed good correlation coefficients (r^2 values of 0.9738 and 0.9086). Receptor occupancy by caffeine (estimated from the slope of the plot) at a dose of 4 mg/kg was 65.9%, and that at

TABLE 2
Biodistribution Data for ^{11}C -MPDX 80 Minutes After Injection

Tissue	SUV for following group:			
	Control (n = 7)	CPA (n = 7)	Caffeine at 4 mg/kg (n = 6)	Caffeine at 40 mg/kg (n = 6)
Amygdala	0.92 ± 0.23	1.29 ± 0.11*	0.69 ± 0.18	0.52 ± 0.08*
Olfactory bulbs	0.70 ± 0.24	0.78 ± 0.21	0.58 ± 0.28	0.43 ± 0.13*
Cerebellum	1.41 ± 0.24	2.23 ± 0.50*	1.10 ± 0.32	0.69 ± 0.15*
Cingulate gyrus	1.11 ± 0.27	1.05 ± 0.22	0.60 ± 0.16*	0.57 ± 0.18*
Entorhinal cortex	1.23 ± 0.33	1.40 ± 0.20	0.66 ± 0.18*	0.59 ± 0.16*
Frontal cortex	1.04 ± 0.26	1.30 ± 0.16*	0.67 ± 0.17*	0.51 ± 0.09*
Hippocampus	1.18 ± 0.25	1.55 ± 0.15*	0.82 ± 0.30*	0.57 ± 0.12*
Medulla	0.90 ± 0.16	1.23 ± 0.28*	0.70 ± 0.17*	0.71 ± 0.20
Parietal, temporal, and occipital cortices	1.19 ± 0.30	1.62 ± 0.39*	0.88 ± 0.24	0.55 ± 0.08*
Pons	0.89 ± 0.27	1.12 ± 0.30	0.72 ± 0.18	0.64 ± 0.24
Striatum	1.13 ± 0.19	1.40 ± 0.20*	0.81 ± 0.23*	0.50 ± 0.07*
Brain tissue left over after dissection	1.17 ± 0.27	1.53 ± 0.34*	0.89 ± 0.28	0.59 ± 0.10*
Bone	0.29 ± 0.14	0.33 ± 0.11	0.32 ± 0.06	0.35 ± 0.05
Colon	0.80 ± 0.30	0.98 ± 0.44	0.90 ± 0.19	1.01 ± 0.22
Duodenum	1.50 ± 0.29	1.63 ± 0.65	1.74 ± 0.56	1.02 ± 0.28*
Fat	1.78 ± 0.43	1.41 ± 0.30	2.37 ± 1.23	1.99 ± 1.02
Heart	0.80 ± 0.14	0.99 ± 0.18	0.91 ± 0.21	0.86 ± 0.15
Ileum	1.24 ± 0.29	1.26 ± 0.38	1.31 ± 0.45	1.12 ± 0.17
Kidneys	1.31 ± 0.15	1.49 ± 0.24	1.19 ± 0.25	1.45 ± 0.21
Liver	2.69 ± 0.49	3.25 ± 0.33*	3.09 ± 0.67	2.74 ± 0.48
Lungs	0.86 ± 0.10	0.87 ± 0.09	0.85 ± 0.14	0.95 ± 0.19
Muscle	0.45 ± 0.06	0.53 ± 0.11	0.54 ± 0.09	0.50 ± 0.12
Pancreas	1.24 ± 0.27	1.37 ± 0.25	1.37 ± 0.48	1.51 ± 0.46
Plasma	0.90 ± 0.11	0.78 ± 0.10	0.92 ± 0.16	0.87 ± 0.17
Red cells	0.42 ± 0.06	0.46 ± 0.08	0.41 ± 0.12	0.47 ± 0.09
Spleen	1.22 ± 0.18	1.15 ± 0.20	0.97 ± 0.20*	0.81 ± 0.18*
Trachea	0.64 ± 0.18	0.66 ± 0.13	0.84 ± 0.20	1.15 ± 0.20*
Urine	0.32 ± 0.39	0.03 ± 0.02	1.14 ± 0.73*	0.40 ± 0.88

*Significantly different from control group.
Data are reported as mean ± SD.

a dose of 40 mg/kg was 98.5%. The V_T for nonspecific binding (estimated from the x -intercept of the plot) was about 0.5, that is, less than 25% of the total V_T s in the target regions with the highest levels of A_1R expression (hippocampus and cerebellum).

DISCUSSION

The drug doses that we administered were based on data reported in the literature. CPA at a dose of 0.25 mg/kg causes a strong hypothermic response in rats that persists for at least 2 h. After repeated administration on subsequent days, a down-regulation of cerebral A_1R that is particularly significant in the hippocampus and somatosensory cortex is observed, and the A_1R system is functionally desensitized (16). Thus, CPA enters the brain and interacts with cerebral A_1R . Caffeine at a dose of 4 mg/kg has been shown to compete with the ligand ^{18}F -FPCPX for binding to adenosine A_1R in the rat brain (14). Although the agonist mass that we injected was an order of magnitude smaller than the mass of the antagonist (0.25 and 4 mg/kg, respectively), in functional terms the agonist dose was much higher because the affinity of CPA for A_1R is in the subnanomolar range (8,9), whereas the affinity of caffeine for A_1R and adenosine A_{2A} receptors is in the 10^{-5} M range (10,11). However, competition between nonradioactive caffeine and ^{11}C -

MPDX for binding to cerebral A_1R was observed, but competition between nonradioactive CPA and the radioligand was not detected.

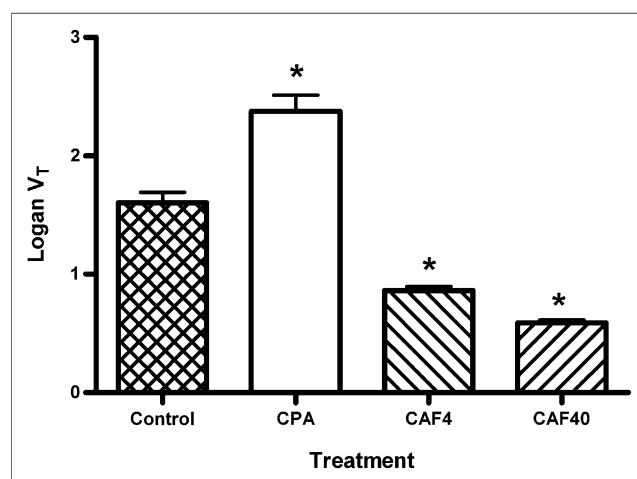


FIGURE 3. V_T of ^{11}C -MPDX in whole brain, calculated from Logan plot. CAF4 = animals treated with caffeine at 4 mg/kg; CAF40 = animals treated with caffeine at 40 mg/kg; CPA = CPA-treated animals. *Significantly different from control group.

A₁R occupancy by caffeine could be calculated from a modified Lassen plot (Fig. 5) (19). A similar plot made from previously published data (7) indicated that the administration of the selective A₁R antagonist DPCPX at 3.2 mg/kg was associated with 100% receptor occupancy. However, the occupancy of A₁R by CPA could not be detected with ¹¹C-MPDX, although the CPA dose that we injected caused a strong decline in the heart rate and was close to the upper limit that could be tolerated by our animals. This observation may indicate that purine agonists and xanthine antagonists interact with the A₁R pharmacophore in different ways. Experiments in which A₁Rs were chemically modified or altered by site-directed mutagenesis indeed showed that agonists and antagonists bind to different domains of the A₁R protein (20,21).

We observed a paradoxical increase in ¹¹C-MPDX binding in the rodent brain after the administration of CPA (Figs. 1, 3, and 4; Table 2). Compartmental analysis of brain time-activity curves with data from arterial plasma samples as an input function indicated that K_1/k_2 values were unchanged but that k_3/k_4 values were elevated after the treatment of animals with CPA (Fig. 4). Similar findings were reported previously for ¹¹C-MPDX in animals that had been treated with ethanol and the adenosine kinase inhibitor ABT702 to increase the endogenous levels of extracellular adenosine (7). These kinetic modeling results suggest that tracer delivery or the passage of ¹¹C-MPDX across the blood-brain barrier is not altered in the presence of CPA (or ethanol

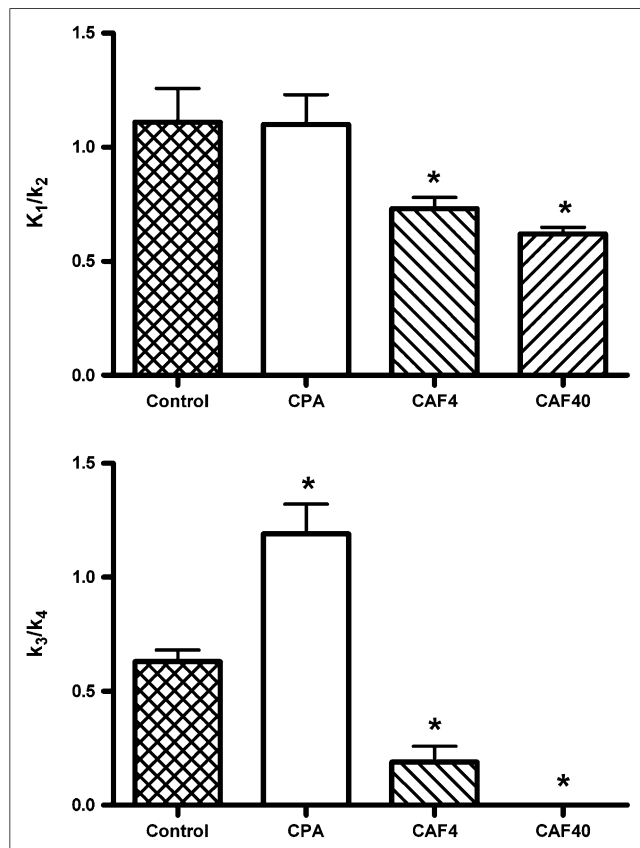


FIGURE 4. Partition coefficient (K_1/k_2) and binding potential (k_3/k_4) for ¹¹C-MPDX in whole brain, calculated from 2TCM fit. CAF4 = animals treated with caffeine at 4 mg/kg; CAF40 = animals treated with caffeine at 40 mg/kg; CPA = CPA-treated animals.

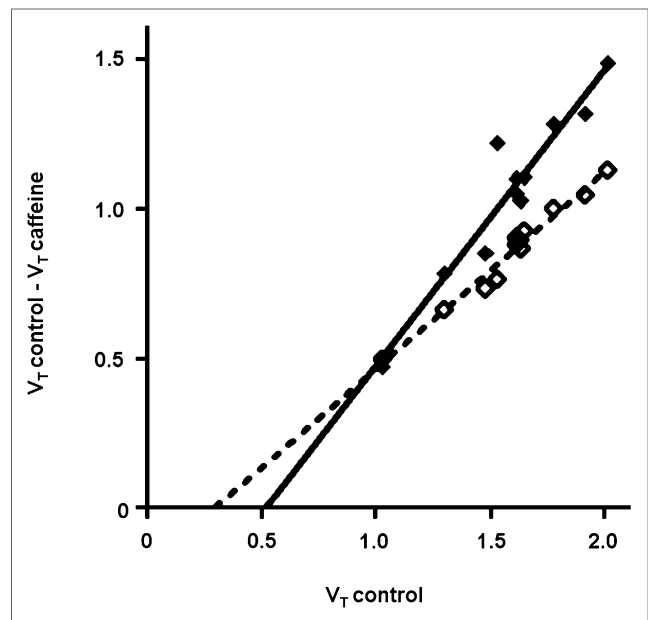


FIGURE 5. Lassen plots for A₁R occupancy by caffeine. \diamond = 4 mg/kg; \blacklozenge = 40 mg/kg.

and ABT702) but that the availability of A₁R or the affinity of A₁R for the radioligand is increased.

The most simple explanation for increased cerebral binding of ¹¹C-MPDX in the presence of CPA or increased levels of extracellular adenosine is the hypothesis that agonists and antagonists bind to different domains on a single A₁R protein or to different protomers in a A₁R homodimer (22), with agonist binding causing a conformational change in the receptor protein (or receptor complex) that facilitates the subsequent binding of an antagonist. Data from a few reports involving isolated biomembranes or brain slices have suggested that A₁R agonists can indeed increase the binding of A₁R antagonists to A₁R (23,24) and vice versa (22).

CONCLUSION

Competition of nonradioactive xanthine antagonists (caffeine and DPCPX) with ¹¹C-MPDX for binding to A₁R in the brains of living rodents was observed with small-animal PET, and values for dose-dependent receptor occupancy could be calculated from a modified Lassen plot (Fig. 5). However, the administration of a high dose of an agonist with a purine structure (CPA) did not result in measurable competition with ¹¹C-MPDX for binding to the target receptor. These data and the data from our previous small-animal PET study with ethanol and ABT702 (7) suggested that agonists and antagonists bind to different sites on the A₁R protein which may show allosteric interactions.

DISCLOSURE

The costs of publication of this article were defrayed in part by the payment of page charges. Therefore, and solely to indicate this fact, this article is hereby marked "advertisement" in accordance with 18 USC section 1734. No potential conflict of interest relevant to this article was reported.

REFERENCES

- Paul S, Elsinga PH, Ishiwata K, Dierckx RA, van Waarde A. Adenosine A₁ receptors in the central nervous system: their functions in health and disease, and possible elucidation by PET imaging. *Curr Med Chem*. 2011;18:4820–4835.
- Elzein E, Zablocki J. A₁ adenosine receptor agonists and their potential therapeutic applications. *Expert Opin Investig Drugs*. 2008;17:1901–1910.
- Noguchi J, Ishiwata K, Furuta R, et al. Evaluation of carbon-11 labeled KF15372 and its ethyl and methyl derivatives as a potential CNS adenosine A₁ receptor ligand. *Nucl Med Biol*. 1997;24:53–59.
- Kimura Y, Ishii K, Fukumitsu N, et al. Quantitative analysis of adenosine A₁ receptors in human brain using positron emission tomography and [1-methyl-¹¹C]8-dicyclopropylmethyl-1-methyl-3-propylxanthine. *Nucl Med Biol*. 2004;31:975–981.
- Holschbach MH, Olsson RA, Bier D, et al. Synthesis and evaluation of no-carrier-added 8-cyclopentyl-3-(3-[¹⁸F]fluoropropyl)-1-propylxanthine ([¹⁸F]CPFPX): a potent and selective A₁-adenosine receptor antagonist for in vivo imaging. *J Med Chem*. 2002;45:5150–5156.
- Bauer A, Holschbach MH, Meyer PT, et al. In vivo imaging of adenosine A₁ receptors in the human brain with [¹⁸F]CPFPX and positron emission tomography. *Neuroimage*. 2003;19:1760–1769.
- Paul S, Khanapur S, Rybczynska AA, et al. Small-animal PET study of adenosine A₁ receptors in rat brain: blocking receptors and raising extracellular adenosine. *J Nucl Med*. 2011;52:1293–1300.
- Moos WH, Szotek DS, Bruns RF. N⁶-cycloalkyladenosines: potent, A₁-selective adenosine agonists. *J Med Chem*. 1985;28:1383–1384.
- Williams M, Braunwalder A, Erickson TJ. Evaluation of the binding of the A-1 selective adenosine radioligand, cyclopentyladenosine (CPA), to rat brain tissue. *Naunyn Schmiedebergs Arch Pharmacol*. 1986;332:179–183.
- Snyder SH, Katims JJ, Annau Z, Bruns RF, Daly JW. Adenosine receptors and behavioral actions of methylxanthines. *Proc Natl Acad Sci USA*. 1981;78:3260–3264.
- Wu PH, Phillis JW, Nye MJ. Alkylxanthines as adenosine receptor antagonists and membrane phosphodiesterase inhibitors in central nervous tissue: evaluation of structure-activity relationships. *Life Sci*. 1982;31:2857–2867.
- Bruns RF, Fergus JH, Badger EW, et al. Binding of the A₁-selective adenosine antagonist 8-cyclopentyl-1,3-dipropylxanthine to rat brain membranes. *Naunyn Schmiedebergs Arch Pharmacol*. 1987;335:59–63.
- Haleen SJ, Steffen RP, Hamilton HW. PD 116,948, a highly selective A₁ adenosine receptor antagonist. *Life Sci*. 1987;40:555–561.
- Meyer PT, Bier D, Holschbach MH, et al. In vivo imaging of rat brain A₁ adenosine receptor occupancy by caffeine. *Eur J Nucl Med Mol Imaging*. 2003;30:1440.
- Elmenhorst D, Meyer PT, Matusch A, Winz OH, Bauer A. Caffeine occupancy of human cerebral A₁ adenosine receptors: in vivo quantification with ¹⁸F-CPFPX and PET. *J Nucl Med*. 2012;53:1723–1729.
- Roman V, Keijsers JN, Luiten PG, Meerlo P. Repetitive stimulation of adenosine A₁ receptors in vivo: changes in receptor numbers, G-proteins and A₁ receptor agonist-induced hypothermia. *Brain Res*. 2008;1191:69–74.
- Schweinhart P, Fransson P, Olson L, Spenger C, Andersson JL. A template for spatial normalisation of MR images of the rat brain. *J Neurosci Methods*. 2003;129:105–113.
- Julien-Dolbec C, Tropres I, Montigon O, et al. Regional response of cerebral blood volume to graded hypoxic hypoxia in rat brain. *Br J Anaesth*. 2002;89:287–293.
- Cunningham VJ, Rabiner EA, Slifstein M, Laruelle M, Gunn RN. Measuring drug occupancy in the absence of a reference region: the Lassen plot re-visited. *J Cereb Blood Flow Metab*. 2010;30:46–50.
- Klotz KN, Lohse MJ, Schwabe U. Chemical modification of A₁ adenosine receptors in rat brain membranes: evidence for histidine in different domains of the ligand binding site. *J Biol Chem*. 1988;263:17522–17526.
- Townsend-Nicholson A, Schofield PR. A threonine residue in the seventh transmembrane domain of the human A₁ adenosine receptor mediates specific agonist binding. *J Biol Chem*. 1994;269:2373–2376.
- Gracia E, Moreno E, Cortes A, et al. Homodimerization of adenosine A₁ receptors in brain cortex explains the biphasic effects of caffeine. *Neuropharmacology*. 2013;71:56–69.
- Olah M, Stiles GL. Agonists and antagonists recognize different but overlapping populations of A₁ adenosine receptors: modulation of receptor number by MgCl₂, solubilization, and guanine nucleotides. *J Neurochem*. 1990;55:1432–1438.
- Schiemann WP, Walther JM, Buxton IL. On the ability of endogenous adenosine to regulate purine nucleoside receptor binding of antagonists in smooth muscle membranes. *J Pharmacol Exp Ther*. 1990;255:886–892.